PROCEEDINGS OF SCIENCE

Lattice calculation of neutral pion decay form factor using two different methods

JLQCD Collaboration: Xu Feng[∗a†], **Sinya Aoki**[b], **Shoji Hashimoto**[a,c], **Takashi Kaneko**[a,c], **Jun-ichi Noaki**[a] **and Eigo Shintani**[d]

[a]*High Energy Accelerator Research Organization (KEK), Tsukuba 305-0801, Japan*
[b]*Graduate School of Pure and Applied Sciences, University of Tsukuba, Tsukuba 305-8571, Japan*
[c]*School of High Energy Accelerator Science, The Graduate University for Advanced Studies (Sokendai), Tsukuba 305-0801, Japan*
[d]*RIKEN-BNL Research Center, Upton, NY 11973-5000, USA*

We perform a non-perturbative study of the two-photon decay of neutral pion using $2+1$ flavors of overlap fermions at pion masses ranging from $m_\pi = 540$ to 300 MeV, at a lattice spacing $a = 0.11$ fm and at a lattice size $L^3 \times T/a^4 = 16^3 \times 48$. Using the all-to-all quark propagator technique, we construct the relevant three-point functions. Using two different methods we compute the $\pi^0 \to \gamma^*\gamma^*$ transition form factor in both space-like and time-like domains. Extrapolating the form factor to the on-shell photon limit, we find that the results from the two methods are consistent.

The XXIX International Symposium on Lattice Field Theory - Lattice 2011
July 10-16, 2011
Squaw Valley, Lake Tahoe, California

[∗]Speaker.
[†]E-mail: xufeng@post.kek.jp

PoS(Lattice 2011)154

1. Introduction

Being the lightest meson, π^0 can not decay to other hadronic states. The principal decay channel (with a branching ratio of 98.8%) of π^0 is to a pair of the photons, which represents one of the key processes in the anomaly sector of gauge field theory. The recent measurement of the $\pi^0 \to \gamma\gamma$ decay width by the PrimEx experiment at JLab gives $\Gamma_{\pi^0\gamma\gamma} = 7.82(22)$ eV [1] and has a fractional accuracy of only 2.8%. Such a precision level makes the π^0 decay to be the most stringent test for the chiral anomaly of gauge theory and its formulation on the lattice.

On the theoretical side, the hadronic aspect of the $\pi^0 \to \gamma\gamma$ transition matrix element is confined in the form factor function $\mathscr{F}_{\pi^0\gamma\gamma}(m_\pi^2, p_1^2, p_2^2)$, where m_π is the π^0 mass and $p_{1,2}$ are the photon momenta. In the case that the photons are on-shell, the constant $\mathscr{F}_{\pi^0\gamma\gamma}(m_\pi^2, 0, 0)$ directly yields the $\pi^0 \to \gamma\gamma$ decay rate through the relation $\Gamma_{\pi^0\gamma\gamma} = (\pi\alpha_e^2 m_\pi^3/4)\mathscr{F}^2_{\pi^0\gamma\gamma}(m_\pi^2, 0, 0)$, where α_e is the fine structure constant. Therefore, by computing $\mathscr{F}_{\pi^0\gamma\gamma}(m_\pi^2, 0, 0)$, we are able to compare the theoretical values of $\Gamma_{\pi^0\gamma\gamma}$ to the experimental measurements.

In the chiral limit, the on-shell photon form factor $\mathscr{F}_{\pi^0\gamma\gamma}(0, 0, 0)$ is predicted by the Adler-Bell-Jackiw (ABJ) anomaly [2, 3, 4] in terms of the π^0 decay constant, F_π, as $\mathscr{F}_{\pi^0\gamma\gamma}(0, 0, 0) = 1/(4\pi^2 F_\pi)$, while some corrections from QCD are expected when the pion is massive or the photons are off-shell. In low energy region the direct determination of these QCD corrections is afflicted with many difficulties since the computation of them is essentially a non-perturbative problem. Lattice QCD provides a genuine non-perturbative method, which can tackle these problems in principle, using numerical simulations.

In the past, two lattice groups have undertaken efforts to study the π^0 decay and the corresponding results are reported in the proceedings [5, 6, 7]. In this work we calculate $F_{\pi^0\gamma\gamma}(m_\pi^2, p_1^2, p_2^2)$ using $N_f = 2+1$ overlap fermion ensembles with fixed topological charge from JLQCD collaboration. As a preliminary calculation, we use two different methods to calculate the form factor and check the consistency of the results. Such a study is useful for the future lattice calculation to finally achieve a precise determination of $\pi^0 \to \gamma\gamma$ transition form factor and pion decay width.

2. Form factor

The $\pi^0\gamma\gamma$ transition form factor $\mathscr{F}_{\pi^0\gamma\gamma}(m_\pi^2, p_1^2, p_2^2)$ is defined through the matrix element

$$\mathscr{F}_{\pi^0\gamma\gamma}(m_\pi^2, p_1^2, p_2^2) = i\int d^4x\, e^{ip_1x}\langle\Omega|T\{j_\mu(x)j_\nu(0)\}|\pi^0(q)\rangle/P_{\mu\nu}(p_1, p_2)\,, \tag{2.1}$$

where q is the π^0 momentum, $p_{1,2}$ are the photon momenta and $j_\mu(x)$ is the electromagnetic vector current. In Eq. (2.1) $P_{\mu\nu}(p_1, p_2) = \varepsilon_{\mu\nu\alpha\beta}p_1^\alpha p_2^\beta$ is a factor of Lorentz structure, induced by the negative parity of the π^0.

Using the LSZ reduction formula and reducing the π^0-state one can rewrite Eq. (2.1) as

$$\mathscr{F}_{\pi^0\gamma\gamma}(m_\pi^2, p_1^2, p_2^2) = \lim_{q^2\to m_\pi^2}\frac{m_\pi^2 - q^2}{\phi_\pi}\int d^4x\, d^4z\, e^{ip_1x-iqz}\langle\Omega|T\left\{j_\mu(x)j_\nu(0)\pi^0(z)\right\}|\Omega\rangle/P_{\mu\nu}(p_1, p_2)\,, \tag{2.2}$$

where ϕ_π is the overlap amplitude, defined as $\phi_\pi = \langle\pi^0(q)|\pi^0(0)|\Omega\rangle = m_\pi^2 F_\pi/(2m_{u,d})$, with $m_{u,d}$ the quark mass.

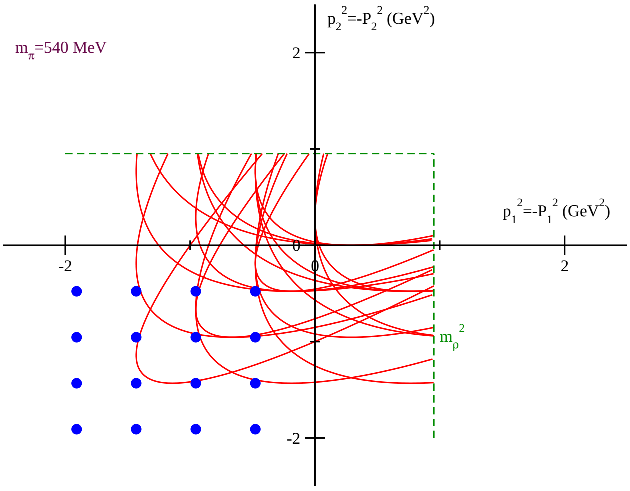

Figure 1: Blue circles and red curves represent the momenta covered by method #1 and #2, respectively.

2.1 Method #1

Eq. (2.2) is originally defined in the Minkowski space-time. Performing the Wick rotation, we obtain a similar formula in the Euclidean space-time

$$\mathscr{F}_{\pi^0\gamma\gamma}(Q^2,P_1^2,P_2^2) = \frac{m_\pi^2+Q^2}{\phi_\pi}\int d^4X\, d^4Z\, e^{-iP_1X+iQZ}\langle\Omega|T\left\{j_\mu(X)j_\nu(0)\pi^0(Z)\right\}|\Omega\rangle/P_{\mu\nu}(P_1,P_2)\,, \quad (2.3)$$

where $P_{1,2}$ and Q are Euclidean momenta and the interpolating operator $j_\mu(X)$, $j_\nu(Y)$ and $\pi^0(Z)$ are defined in the Euclidean space-time. We apply Eq. (2.3) to the lattice QCD calculation. As shown by the blue circles in Fig. 1, using Eq. (2.3), we obtain the form factor in the space-like momentum region with photon momenta $p_{1,2}^2 = -P_{1,2}^2 < 0$.

Note that in Eq. (2.2) the limit $q^2 \to m_\pi^2$ should be taken. However, in Eq. (2.3) the pion momenta are always space-like and never hit the pion pole. Therefore the "form factor" defined in Eq. (2.3) is that for an off-shell pion. In our calculation we concentrate on the small $|q^2|$ region, so that the π^0 is not very far away from its pole and the off-shell amplitude may give a reasonable approximation to the on-shell form factor.

2.2 Method #2

Besides using Eq. (2.3) we can also make use of Ji and Jung's method to calculate the form factor [8]. We analytically continue Eq. (2.1) from the Minkowski to Euclidean space-time. After the continuation, we have

$$\mathscr{F}_{\pi^0\gamma\gamma}(m_\pi^2,p_1^2,p_2^2) = \int dt\, e^{\omega t}\int d^3\vec{x}\, e^{-i\vec{p}_1\cdot\vec{x}}\langle\Omega|T\{j_\mu(\vec{x},t)j_\nu(\vec{0},0)\}|\pi^0(q)\rangle/P_{\mu\nu}(p_1,p_2)\,. \quad (2.4)$$

In Eq. (2.4) the pion has momentum $q = (E_{\pi,\vec{q}},\vec{q})$, which satisfies the on-shell condition $q^2 = m_\pi^2$. The first photon has momentum $p_1 = (\omega,\vec{p}_1)$, where the photon energy ω is put by hand and can be tuned continuously. According to the momentum conservation, the second photon's momentum is given as $p_2 = (E_{\pi,\vec{q}} - \omega, \vec{q} - \vec{p}_1)$. Fixing the values for spatial momenta $\vec{q}$ and $\vec{p}$ and tuning the value for ω, we find that (p_1^2, p_2^2), with $p_1^2 = \omega^2 - \vec{p}_1^2$ and $p_2^2 = (E_{\pi,\vec{q}} - \omega)^2 - (\vec{q} - \vec{p}_1)^2$, forms continuous contours on the (p_1^2, p_2^2) plane. (See the red curves in Fig. 1 as an example.) With an appropriate choice for ω, the photons can be space-like or time-like. Although possibly time-like, the photons should not hit the poles of hadrons. Otherwise, the photon states may mix with the hadron states and it is not allowed to analytically continue Eq. (2.1) from the Minkowski to Euclidean space-time. To avoid such situation we keep $p_{1,2}^2 < m_\rho^2$ (or $E_{\pi\pi}^2$ depending on quark masses), where the upper limit refers to the hadron production threshold.

3. Lattice setup

In this work we use the $N_f = 2+1$ overlap fermion configurations from the JLQCD collaboration. Using the overlap fermions ensures the exact chiral symmetry at finite lattice spacings. The results presented here are from a sequence of ensembles with a lattice spacing of $a = 0.11$ fm and a lattice size of $L^3 \times T/a^4 = 16^3 \times 48$. There are four pion masses used in the calculation: $m_\pi = 540$, 460, 380 and 300 MeV. At the smallest two pion masses with $m_\pi L = 2.8$ and 3.5, the finite size effect might be significant to the data.

To calculate the form factor, we construct a three-point correlation function

$$C_{\mu\nu}(t_1, t_2, t_\pi) = \frac{1}{V} \langle j_\mu(\vec{p}_1, t_1) j_\nu(\vec{p}_2, t_2) \pi^0(-\vec{q}, t_\pi) \rangle \,, \tag{3.1}$$

where j_μ is the Fourier-Transformed local vector current. The renormalization factor Z_V is added to j_μ so that the lattice results can match the continuum theory. The spatial momenta of the photons and π^0 are set as $\vec{p}_1 = (2\pi/L)(0,0,0)$, $\vec{p}_2 = (2\pi/L)(0,0,1)$ and $\vec{q} = (2\pi/L)(0,0,1)$.

We use the all-to-all propagator technique to calculate the correlator. The low-lying eigenmodes of the propagators are prepared in advance. The high modes are extracted from the stochastic propagators. Using all-to-all propagators allows us to calculate $C_{\mu\nu}(t_1, t_2, t_\pi)$ at any time slice of t_1, t_2 and t_π with good statistical precision. For more details we refer readers to Refs. [9, 10].

Using $C_{\mu\nu}(t_1, t_2, t_\pi)$ as an input, the method #1 gives

$$\mathscr{F}_{\pi^0\gamma\gamma}(Q^2, P_1^2, P_2^2) = \frac{m_\pi^2 + Q^2}{\phi_\pi} \frac{1}{T} \sum_{t_1, t_2, t_\pi} e^{iP_{10}t_1} e^{iP_{20}t_2} e^{-iQ_0 t_\pi} C_{\mu\nu}(t_1, t_2, t_\pi) / P_{\mu\nu}(P_1, P_2) \,, \tag{3.2}$$

with Euclidean momenta $P_1 = (\vec{p}_1, P_{10})$, $P_2 = (\vec{p}_1, P_{20})$ and $Q = (\vec{q}, Q_0)$. The method #2 yields

$$\mathscr{F}_{\pi^0\gamma\gamma}(m_\pi^2, p_1^2, p_2^2) = \int dt_1\, e^{\omega(t_1 - t_2)} C_{\mu\nu}(t_1, t_2, t_\pi) / \left(\frac{\phi_\pi}{2E_{\pi,\vec{q}}} e^{-E_{\pi,\vec{q}}(t_2 - t_\pi)} \right) / P_{\mu\nu}(p_1, p_2) \,, \tag{3.3}$$

with Minkowski momenta $p_1 = (\omega, \vec{p}_1)$, $p_2 = (E_{\pi,\vec{q}} - \omega, \vec{p}_2)$ and $q = (E_{\pi,\vec{q}}, \vec{q})$.

4. Extract the ground state of π^0

To eliminate the pseudo-scalar (PS) excited-state effects in the method #2, we first look at the correlator $C_{\mu\nu}(t_1, t_2, t_\pi)$ in Eq. (3.1) at $t_1 = t_2 = t$. At large $t - t_\pi$, where the excited-state effects are highly suppressed, the correlators are dominated by the π^0-ground state as

$$\lim_{t - t_\pi \to \infty} C_{\mu\nu}(t, t, t_\pi) = A_\pi e^{-E_{\pi,\vec{q}}(t - t_\pi)} \,, \quad A_\pi = \frac{1}{V} \frac{\phi_\pi}{2E_{\pi,\vec{q}}} \langle \Omega | j_\mu(\vec{p}_1, 0) j_\nu(\vec{p}_2, 0) | \pi^0(\vec{q}) \rangle \,. \tag{4.1}$$

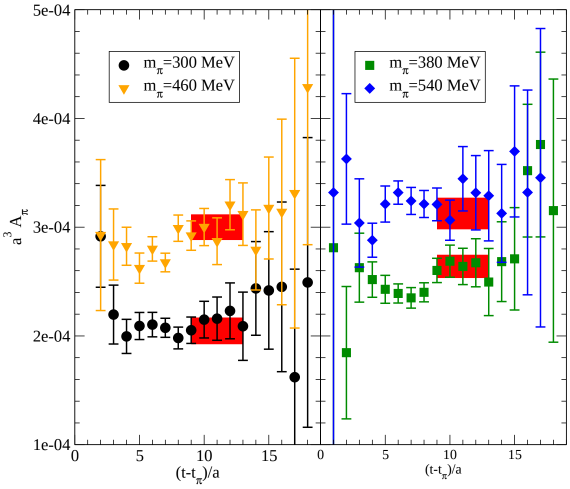

Figure 2: A_π as a function of $t-t_\pi$ together with a correlated fit to a constant value.

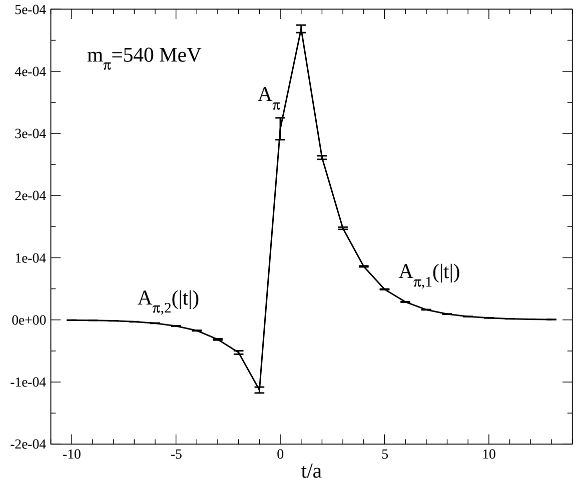

Figure 3: At $m_\pi = 540$ MeV $A_{\pi,1}(|t|)$ as a function of t for $t>0$ and $A_{\pi,2}(|t|)$ as a function of t for $t<0$.

The corresponding results for $A_\pi = C_{\mu\nu}(t,t,t_\pi)/e^{-E_{\pi,\vec{q}}(t-t_\pi)}$ as a function of $t-t_\pi$ are shown in Fig. 2. At large $t-t_\pi$ we expect a plateau for A_π, while at small $t-t_\pi$ such constant behavior can be distorted by the excited-state effects. As shown in Fig. 2, we do not observe strong excited-state effects. By choosing appropriate fitting windows, we fit A_π to a constant value. The corresponding fitting curves are shown in Fig. 2.

As a next step, we consider the cases for $t_1 \neq t_2$. We keep $t_{1,2} > t_\pi$ to ensure the π^0-state be the initial state. Let $\Delta t = |t_1 - t_2|$ and $t = \min\{t_1, t_2\}$. At large $t-t_\pi$, the correlators can be written as

$$\begin{aligned}
\lim_{t-t_\pi\to\infty} C_{\mu\nu}(t+\Delta t, t, t_\pi) &= A_{\pi,1}(\Delta t) e^{-E_{\pi,\vec{q}}(t-t_\pi)}\ , \quad \text{for } t_1 > t_2\ , \\
\lim_{t-t_\pi\to\infty} C_{\mu\nu}(t, t+\Delta t, t_\pi) &= A_{\pi,2}(\Delta t) e^{-E_{\pi,\vec{q}}(t-t_\pi)}\ , \quad \text{for } t_2 > t_1\ ,
\end{aligned} \tag{4.2}$$

with

$$\begin{aligned}
A_{\pi,1}(\Delta t) &= \frac{1}{V}\frac{\phi_\pi}{2E_{\pi,\vec{q}}} \langle \Omega | j_\mu(\vec{p}_1, \Delta t) j_\nu(\vec{p}_2, 0) | \pi^0(\vec{q}) \rangle\ , \\
A_{\pi,2}(\Delta t) &= \frac{1}{V}\frac{\phi_\pi}{2E_{\pi,\vec{q}}} \langle \Omega | j_\nu(\vec{p}_2, \Delta t) j_\mu(\vec{p}_1, 0) | \pi^0(\vec{q}) \rangle\ .
\end{aligned} \tag{4.3}$$

Given each value of Δt, $A_{\pi,1,2}(\Delta t)$ is a function of $t-t_\pi$. We choose the appropriate fitting windows to fit $A_{\pi,1,2}(\Delta t)$ to a constant value. Take the ensemble with $m_\pi = 540$ MeV as an example. Using the fitted results for $A_{\pi,1,2}(\Delta t)$ at different Δt, we make a plot in Fig. 3 for $A_{\pi,1}(|t|)$ as a function of t for $t>0$ and $A_{\pi,2}(|t|)$ as a function of t for $t<0$.

5. Results

Based on the observation that the PS excited-state effects are not significant, using the method #1 we calculate the form factor directly from Eq. (3.2). At $m_\pi = 540$ MeV the result for the normalized form factor $4\pi^2 F_\pi \mathscr{F}_{\pi^0\gamma\gamma}(Q^2, P_1^2, P_2^2)$ as a function of $p_2^2 = -P_2^2$ is shown in Fig. 4.

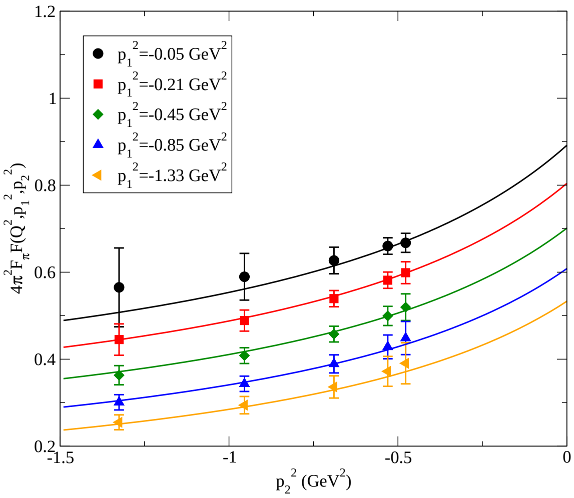

Figure 4: At $m_\pi = 540$ MeV normalized form factor calculated from method #1 as a function of momenta p_2^2. The momenta are restricted in space-like domain.

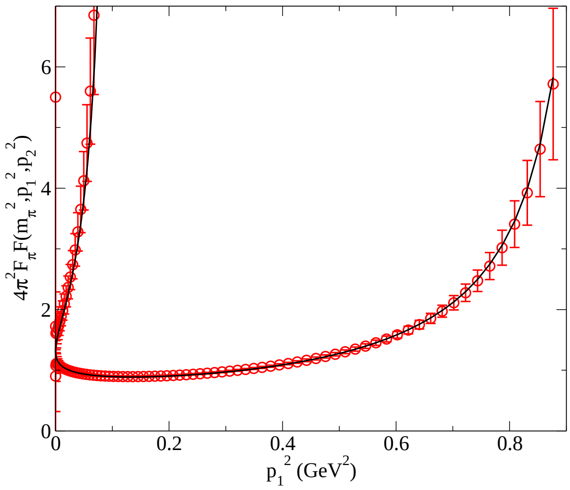

Figure 5: At $m_\pi = 540$ MeV normalized form factor calculated from method #2 as a function of momenta p_1^2. The momenta p_1^2 are the time-like momenta.

When using the method #2, since we have extracted the amplitude A_π and $A_{\pi,1,2}$, we put them into Eq. (3.3) and calculate the form factor through

$$\mathscr{F}_{\pi^0\gamma\gamma}(m_\pi^2, p_1^2, p_2^2) = \frac{2E_{\pi,\vec{q}}}{\phi_\pi}\left(\int_0^\infty dt\, e^{\omega t} A_{\pi,1}(|t|) + \int_{-\infty}^0 dt\, e^{(\omega - E_{\pi,\vec{q}})t} A_{\pi,2}(|t|)\right) / P_{\mu\nu}(p_1, p_2)\,. \tag{5.1}$$

Eq. (5.1) requires an integral interval of $t \in (-\infty, \infty)$. However, on lattice the available intervals are always truncated due to the finite total time extent T. Our solution is as follows. At large $|t|$, although lattice data are unavailable, the long-distance behavior of the integrand is known: It is dominated by the ground state. Therefore by extrapolating the integrand to the large $|t|$ region we can accomplish the integration from $t = -\infty$ to $t = +\infty$. At $m_\pi = 540$ MeV the result for $4\pi^2 F_\pi \mathscr{F}_{\pi^0\gamma\gamma}(m_\pi^2, p_1^2, p_2^2)$ as a function of p_1^2 is shown in Fig. 5.

After determining the form factors at diferent momenta $p_{1,2}^2$, the next step is to extrapolate them to the on-shell photon limit $p_{1,2}^2 = 0$. Here we employ a fit ansatz

$$\begin{aligned}\mathscr{F}_{\pi^0\gamma\gamma}(m_\pi^2, p_1^2, p_2^2) &= c_V G_V(p_1^2) G_V(p_2^2) + \\ &\sum_m c_m \left((p_1^2)^m G_V(p_2^2) + (p_2^2)^m G_V(p_1^2)\right) + \sum_{m,n} c_{m,n} (p_1^2)^m (p_2^2)^n\,,\end{aligned} \tag{5.2}$$

where $G_V(p^2) = M_V^2/(M_V^2 - p^2)$ is the vector meson propagator with M_V the vector meson mass. We fit the data of the form factor to Eq. (5.2) with four free parameters: c_V, c_0, $c_{0,0}$ and $c_{1,0}$. The fitting curves are shown in Figs. 4 and 5. For both methods #1 and #2, the fits work well.

The normalized on-shell form factors are shown as a function of m_π^2 in Fig. 6. We find that the results from the two different methods are consistent.

Although the results reported here are still preliminary, the consistency between the two different methods suggests that our calculation is fairly reliable. However, as shown in Fig. 6, at smallest pion mass, we find that normalized form factor is much less than the value predicted by the ABJ anomaly, which is unity in the chiral limit. We will further investigate this problem.

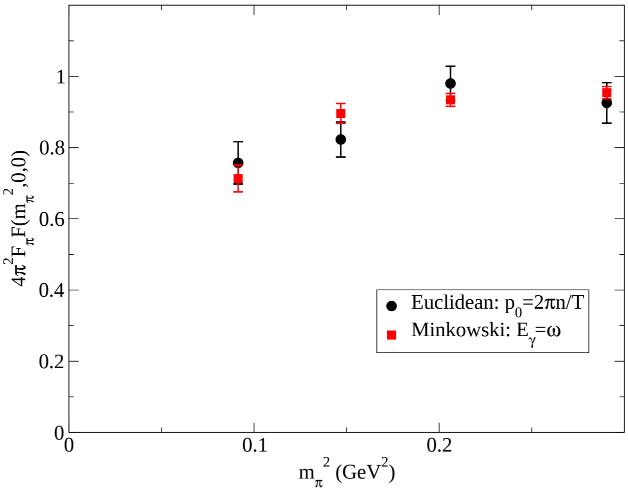

Figure 6: Normalized on-shell form factor as a function of m_π^2. The results from the two different methods are statistically consistent.

We thank our fellow members of JLQCD collaboration for discussion and feedback throughout the course of this work. Numerical simulations are performed on the Hitachi SR16000 at Yukawa Institute of Theoretical Physics (YITP) and the IBM System Blue Gene Solution at High Energy Accelerator Research Organization (KEK) under a support of its Large Scale Simulation Program (No. 10-11). This work is supported in part by the Grant-in-Aid of the Japanese Ministry of Education (No.21674002, 21684013), the Grant-in-Aid for Scientific Research on Innovative Areas (No. 2004: 20105002, 20105005), and the HPCI Strategic Program of Ministry of Education.

References

[1] I. Larin et al. *Phys. Rev. Lett.*, 106:162303, 2011.

[2] S. L. Adler. *Phys. Rev.*, 177:2426–2438, 1969.

[3] J. S. Bell and R. Jackiw. *Nuovo Cim.*, A60:47–61, 1969.

[4] S. L. Adler and W. A. Bardeen. *Phys. Rev.*, 182:1517–1536, 1969.

[5] S. D. Cohen, H. W. Lin, J. Dudek, and R. G. Edwards. *PoS*, LAT2008:159, 2008.

[6] E. Shintani, S. Aoki, S. Hashimoto, T. Onogi, and N. Yamada. *PoS*, LAT2009:246, 2009.

[7] E. Shintani, S. Aoki, S. Hashimoto, T. Onogi, and N. Yamada. *PoS*, LAT2010:159, 2010.

[8] X. D. Ji and C. W. Jung. *Phys. Rev. Lett.*, 86:208, 2001.

[9] J. Foley et al. *Comput.Phys.Commun.*, 172:145–162, 2005.

[10] S. Aoki et al. *Phys. Rev.*, D80:034508, 2009.